Received September 29, 2020, accepted November 6, 2020, date of publication November 10, 2020,
date of current version November 20, 2020.

Digital Object Identifier 10.1109/ACCESS.2020.3037069

Max-Min Throughput in Hybrid of Wireless Powered NOMA and Backscatter Communications

WEN-GANG ZHOU
School of Computer Science and Technology, Zhoukou Normal University, Zhoukou 466001, China
Macau Big Data Research Centre, City University of Macau, Taipa, Macao
e-mail: zhouwengang@zknu.edu.cn

ABSTRACT This article proposes a hybrid of backscatter communication (BackCom) and wireless powered non-orthogonal multiple access (NOMA) network for Internet of Things (IoT) applications, which consists of one power beacon (PB), multiple energy-constrained IoT devices, and one information receiver (IR). In the proposed network, the IoT devices harvest energy and backscatter their information to the IR in turn when PB broadcasts energy signals, and then use the harvested energy to transmit information to the IR via uplink NOMA when PB keeps silent. Considering the non-overflowing energy constraint, a max-min throughput optimization problem is formulated to ensure the throughput fairness among different IoT devices by jointly optimizing the time resource for operating BackCom and uplink NOMA, the reflection coefficient of BackComs, the transmit power for uplink NOMA and the transmit power of the PB. Although the formulated problem is non-convex and challenging to solve, we first transform the original non-convex problem into an equivalent convex one with the aid of an inequality transformation approach and introducing several kinds of auxiliary variables, and then devise a two-layer iterative algorithm to obtain the optimal resource allocation. Simulation results are provided to verify the convergence of the devised iterative algorithm and validate that the proposed scheme achieves the highest max-min throughput by comparing it with three baseline schemes.

INDEX TERMS Wireless powered non-orthogonal multiple access, backscatter communication, max-min throughput.

I. INTRODUCTION

In the era of Internet of Things (IoT), there will be ultra-massive battery-power IoT devices deployed in various communication systems, e.g., intelligent automatic manufacturing system, to monitor, and report data to the information fusion for realizing intelligent IoT services [1]. Due to the stringent device size constraint and production cost consideration, the battery capacity of the IoT device is usually very small and hence the limited operation time of the IoT device becomes one of major challenges for the applications of IoT. Wireless information and power transfer (WIPT) has been considered as a potential solution for this challenge and has attracted much attention in the recent years, due to the ability to realize information transfer and energy harvesting (EH) in each transmission block [2]–[5].

The associate editor coordinating the review of this manuscript and approving it for publication was Muhammad Khandaker.

Wireless powered communication network (WPCN) [6]–[9] and wireless powered backscattter communication (BackCom) [4], [10]–[13] are two popular types in the field of WIPT. In WPCN, the IoT device first harvests energy from the radio frequency (RF) signals transmitted by the RF source, e.g., power beacon (PB), and then follows the ''harvest-then-transmit'' protocol conveying its own message to its associated receiver via active transmissions, where the IoT device needs to generate the carrier signal and modulate its own message on the generated carrier [6]–[9]. Accordingly, the realization of active transmissions requires energy-consuming active components, e.g., oscillator and A/D converter, leading to a high power consumption. In order to harvest sufficient energy for active transmissions, the transmitter, in WPCNs, should allocate a long period within the time block for EH, leaving a short period within the time block for active transmissions, and this limits the its achievable throughput. Different from the WPCN, in BackComs,

the transmitter splits the incoming signal transmitted by a carrier emitter into two parts based on a reflection coefficient: one is used as a carrier signal for modulating its own message and then is backscattered towards its associated receiver, and the other is fed into the energy harvester for EH so as to operate its circuit [11], [13]. Accordingly, the transmitter in BackComs bypasses the need of energy-consuming active components for generating carrier signals and BackCom is recognized as an ultra low-power communication technology. Due to different operation principles, WPCN and BackCom have different tradeoffs between the achievable rate and the energy consumption, i.e., BackCom achieves much less rate but consumes much less energy compared with WPCN [4], [14].

Recently, the above two technologies, WPCN and BackCom, have been linked together for effectively inheriting their advantages [15]–[18]. In [15], the authors studied a point-to-point communication network, where the IoT device conveys information to the information fusion via backscattering the received signals or active transmissions. In such a case, a joint time and reflection coefficient allocation scheme was proposed to maximize the achievable throughput. In [16] and [17], the authors considered a cognitive radio (CR) network with one secondary link and one primary link, where the secondary transmitter (ST) operates in a hybrid of WPCN and BackCom mode for conveying information to the secondary receiver (SR). Subsequently the EH time, BackCom's time, and the active transmission's time was jointly optimized to maximize the achievable throughput of a secondary link while ensuring the required throughput of the primary link. Focusing on the energy efficiency (EE) maximization instead of the throughput maximization, the authors of [18] studied a joint time resource and detection threshold allocation scheme in a CR network with hybrid of WPCN and BackCom.

Different from the above works only considering a single ST [15]–[18], several works with the focus on the design of resource allocation schemes for the multiple STs scenario have been expended [19]–[26]. In [19], the authors proposed a sum-throughput maximization based time resource allocation scheme for a CR network with one primary link and multiple secondary links. Considering a similar network with [19] while deploying one PB nearly with the secondary transmitters to further boost the throughput, the authors in [20] proposed a novel time resource allocation scheme to maximize the sum-throughput of the secondary links. In [21], using the tool from Stackelberg game, the time resource was optimized to maximize the utilities of secondary links and primary link, respectively. In contrast to [19]–[21], the authors in [23] and [24] investigated the sum-throughput maximization based resource allocation problem in wireless powered sensor networks, where the IoT devices report their data to the information fusion via the hybrid of WPCN and BackCom. Since the sum-throughput maximization is usually at the cost of decreasing the fairness among different IoT devices, a max-min approach was considered and an optimal joint of reflection coefficients and time allocation scheme was developed to maximize the minimal throughput. Considering the EE instead of the throughput maximization in [19]–[25], the EE of all IoT devices was maximized by jointly optimizing the power and time resource [26]. Despite the research progress, all the prior works [19]–[26] considered that all IoT devices adopt orthogonal multiple access (OMA) schemes for active transmissions. That is, these works focused on the backscatter-assisted wireless powered OMA network. Such a combination, however, may not meet the requirements simultaneously in terms of throughput and fairness particularly when the channel conditions from IoT devices to the information fusion are significantly different, and this motivates us to consider another multiple access scheme for active transmissions.

Recently, it has been validated that compared with the OMA, non-orthogonal multiple access (NOMA) scheme, one of novel multiple access schemes, achieves a larger throughput of the system while ensuring the fairness among transmission links. Thanks to this advantage, various contributions (see [27]–[29] and reference therein) have been devoted to designing resource allocation schemes to satisfy different goals for wireless powered NOMA networks, where multiple IoT devices harvest energy firstly and then transmit their information to the information fusion via uplink NOMA. Recall that the integration of BackCom and wireless powered OMA can bring a significant performance gain, but until now, there is no open work to study the backscatter assisted wireless powered NOMA and hence it is still unclear about how much performance gain it could provide, as compared with the wireless powered NOMA, BackCom, and backscatter assisted wireless powered OMA.

In this article, we aim to respond the above questions and reveal the advantage of the combination of wireless powered NOMA and BackCom. More specifically, we consider a backscatter assisted wireless powered NOMA network, where multiple energy-constrained IoT devices are powered by the RF signals emitted by the PB, and employ hybrid of BackCom and uplink NOMA to report their information to the information receiver (IR).

The contributions of this article are summarized as follows.

- We study the throughput maximization under the max-min fairness criterion for backscatter assisted wireless powered NOMA networks to ensure the throughput fairness among different IoT devices. In particular, we propose a scheme to maximize the minimum throughput of IoT devices by jointly optimizing the transmit power of the PB, the backscatter time and reflection coefficients of IoT devices, the time and the transmit power of IoT devices for uplink NOMA. This joint optimization is formulated into a non-convex problem, which is quite difficult to solve.
- To solve the formulated non-convex problem, we first employ an inequality transformation approach to transform it into an equivalent problem and then introduce several kinds of auxiliary variables to convert the transformed problem as a convex problem.

A two-layer iterative algorithm is devised to obtain the optimal resource allocation scheme. Besides, we derive closed-form expressions for the optimal transmit power and reflection coefficients of IoT devices. It shows that when the IoT device works in the hybrid of wireless powered NOMA and BackCom, the IoT device should consume all the harvested energy or adopt the maximum transmit power for achieving the max-min throughput.

- Simulation results illustrate the convergence of the proposed algorithm and show that the proposed scheme can greatly improve throughput fairness among IoT devices by comparing it with three baseline schemes, which demonstrates the superiority of the combination of wireless powered NOMA and BackCom.

II. SYSTEM MODEL

As shown in Fig. 1, this article considers an uplink IoT network, where M IoT devices need to report their data to a remote IR. In order to prolong the operation time of IoT devices, one PB is deployed nearly with M IoT devices for providing energy signals on demand. We assume that each IoT device is equipped with the EH circuit, the backscatter circuit and the active radio circuit so that they can work in a hybrid WPCN and BackCom mode. Let $h_{\mathrm{P},i}$, $h_{i,j}$, and $h_{i,\mathrm{R}}$ denote the channel gains of the PB-to-the i-th IoT device link, the i-th IoT device-to-the j-th IoT device link, the i-th IoT device-to-IR link, respectively, where $i, j = 1, 2, \ldots, M$ and $i \neq j$. A quasi-static fading is considered and the entire transmission block with the duration of T seconds is less than the channel coherence interval, which means that the channel

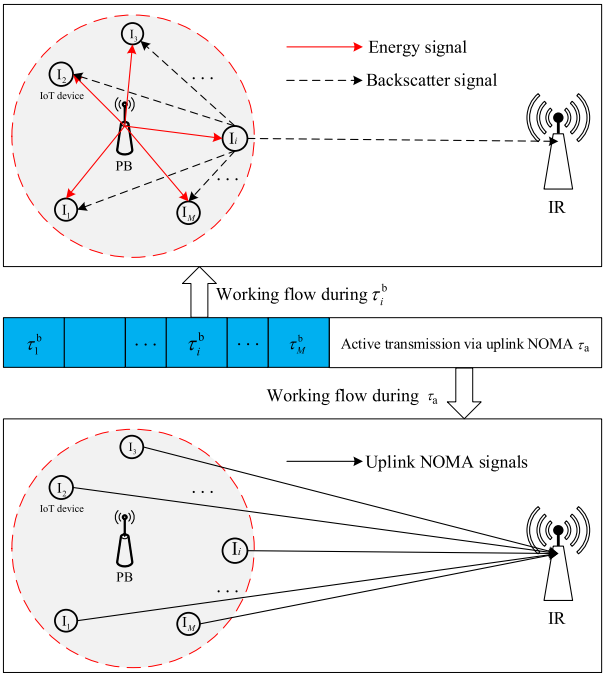

FIGURE 1. Wireless powered IoT network and its time scheduling structure.

gains $h_{\mathrm{P},i}$, $h_{i,j}$, and $h_{i,\mathrm{R}}$ remain unchanged within a given transmission block T and may vary independently between different transmission blocks. Here we assume that all the channels undergo independent identically distributed (i.i.d) Rayleigh fading.

The entire transmission block T is divided into two main phases, namely backscatter phase and uplink NOMA phase. During the whole backscatter phase, the PB keeps broadcasting predefined signals to all the IoT devices while the PB will keep silent in the uplink NOMA phase. The backscatter phase is further divided into M slots,[1] i.e., $\{\tau_i^{\mathrm{b}}, i = 1, 2, \ldots, M\}$. In the sub-phase τ_i^{b}, the i-th IoT device works in the backscatter mode, where its received signal will be split into two parts based on its reflection coefficient α_i ($0 \leq \alpha_i \leq 1$). Specifically, one part with a α_i portion of the received power is backscattered to the IR carrying some information and the rest is flowed into the EH circuit so as to support its circuit operation. Please note that when the i-th IoT device backscatters information to the IR, the other IoT devices will work in the EH mode, where the RF signals from both the PB and the i-th IoT device are harvested.

Assume that successive interference cancellation[2] (SIC) is performed at the IR to remove the interference caused by the PB-to-IR link. Let P_{s} denote the transmit power at the PB. After applying SIC, the achievable throughput at the IR during the sub-phase τ_i^{b} is given by

$$R_i^{\mathrm{b}} = B\tau_i^{\mathrm{b}} \log_2 \left(1 + \frac{\xi \varepsilon_i \alpha_i P_{\mathrm{s}} h_{\mathrm{P},i} h_{i,\mathrm{R}}}{B\sigma^2}\right), \tag{1}$$

where B is the system bandwidth, σ^2 denotes the thermal noise power spectral density, $\varepsilon_i \in (0, 1)$ is the scattering efficiency of the transmit antenna at the i-th IoT device [22], [30] and ξ ($0 \leq \xi \leq 1$) reflects the performance gap between the BackCom and the active transmission [14], [25], [26]. Correspondingly, the harvested energy at the i-th IoT device in this sub-phase can be computed as

$$E_i^{\mathrm{H}} = \eta_i (1 - \alpha_i) P_{\mathrm{s}} h_{\mathrm{P},i} \tau_i^{\mathrm{b}}, \tag{2}$$

where $\eta_i \in (0, 1)$ is the energy conversion efficiency of the EH circuit at the i-th IoT device. In practice, the energy harvester is non-linear but when the input power is low, the non-linear EH model can be approximated as a linear one, and the linear EH will simply the optimization problem. Accordingly, for analytical tractability, many related works, e.g., [19]–[24], adopted a linear EH model instead of the

[1] The practical backscatter transmitter is usually low cost and its backscatter circuit is also simple. Due to this, backscatter transmitter may not support the mode where multiple IoT devices operate in the backscatter mode within the same resource block. Accordingly, we adopt a TDMA scheme and let IoT devices backscatter its information in turn.

[2] In this work, the reasons for assuming perfect CSI during BackCom and uplink NOMA are twofold. Firstly, this assumption has been widely used in related works (please see [25], [27] and reference therein) and can simply the optimization problem. Secondly, such an assumption can obtain a upper bound of max-min throughput in the considered network. Relaxing this assumption into imperfect CSI makes the considered network more realistic, which can be viewed as an interesting topic in the future.

non-linear EH model, and this motivates us to make this assumption.

As for the j-th ($\{j, j = 1, 2, \ldots, M, j \neq i\}$) IoT device, it harvests energy from the energy signals transmitted by the PB and the backscattered signals from i-th IoT device. As a result, the harvested energy of the j-th IoT device in this sub-phase can be calculated as

$$E_{i,j}^{\mathrm{H}} = \eta_j \left(P_{\mathrm{s}} h_{\mathrm{P},j} + \alpha_i P_{\mathrm{s}} h_{\mathrm{P},i} h_{i,j}\right) \tau_i^{\mathrm{b}}. \tag{3}$$

Accordingly, at the end of the backscatter phase, the total harvested energy at the i-th IoT device is given by

$$\begin{aligned} E_{\mathrm{total}}^{i} &= E_i^{\mathrm{H}} + \sum_{j=1, j\neq i}^{M} E_{j,i}^{\mathrm{H}} \\ &= \sum_{j=1, j\neq i}^{M} \eta_i \left(P_{\mathrm{s}} h_{\mathrm{P},i} + \alpha_j P_{\mathrm{s}} h_{\mathrm{P},j} h_{j,i}\right) \tau_j^{\mathrm{b}} \\ &\quad + \eta_i \left(1 - \alpha_i\right) P_{\mathrm{s}} h_{\mathrm{P},i} \tau_i^{\mathrm{b}}. \end{aligned} \tag{4}$$

During the uplink NOMA phase of duration τ_{a}, the M IoT devices will transmit their information to the IR simultaneously via uplink NOMA. In this work, we adopt the following SIC order,[3] i.e., the IR will decode the message transmitted by the IoT device with the best channel condition first, subtract the decoded message from the received composite signal, and then continue to decode the message transmitted by the IoT device with the next best channel condition [27]–[29]. On this basis, we assume that the channel gains between the IoT devices and the IR are ranked in a descending order, i.e., $h_{1,\mathrm{R}} \geq h_{2,\mathrm{R}} \geq \ldots \geq h_{M,\mathrm{R}}$. Let c_i denote the message transmitted by the i-th IoT device in the uplink NOMA phase. Then, the IR will decode c_i first, subtract it from the received composite signal, and continue to decode c_{i+1}, until all M received messages are decoded. Let p_i denote the transmit power of the i-th IoT device in the uplink NOMA phase. Then the achievable throughput of the i-th IoT device in this phase is given by

$$\begin{aligned} R_i^{\mathrm{a}} &= B\tau_{\mathrm{a}} \\ &\times \begin{cases} \log_2\left(1 + \dfrac{p_i h_{i,\mathrm{R}}}{\sum\limits_{m=i+1}^{M} p_m h_{m,\mathrm{R}} + B\sigma^2}\right), & \text{if } i \leq M-1, \\ \log_2\left(1 + \dfrac{p_M h_{M,\mathrm{R}}}{B\sigma^2}\right), & \text{if } i = M. \end{cases} \end{aligned} \tag{5}$$

Based on (5), the total achievable throughput of the i-th IoT device in the entire transmission block can be computed as

$$\begin{aligned} &R_i^{\mathrm{tot}} \\ &= R_i^{\mathrm{b}} + R_i^{\mathrm{a}} \\ &= \begin{cases} B\tau_i^{\mathrm{b}} \log_2\left(1 + \dfrac{\xi \varepsilon_i \alpha_i P_{\mathrm{s}} h_{\mathrm{P},i} h_{i,\mathrm{R}}}{B\sigma^2}\right) \\ \quad + B\tau_{\mathrm{a}} \log_2\left(1 + \dfrac{p_i h_{i,\mathrm{R}}}{\sum\limits_{m=i+1}^{M} p_m h_{m,\mathrm{R}} + B\sigma^2}\right), & \text{if } i \leq M-1, \\ B\tau_i^{\mathrm{b}} \log_2\left(1 + \dfrac{\xi \varepsilon_i \alpha_i P_{\mathrm{s}} h_{\mathrm{P},i} h_{i,\mathrm{R}}}{B\sigma^2}\right) \\ \quad + B\tau_{\mathrm{a}} \log_2\left(1 + \dfrac{p_M h_{M,\mathrm{R}}}{B\sigma^2}\right), & \text{if } i = M. \end{cases} \end{aligned} \tag{6}$$

III. THROUGHPUT FAIRNESS BASED RESOURCE ALLOCATION

A. PROBLEM FORMULATION

In this work, we aim to maximize the achievable throughput of IoT devices under the max-min fairness criterion by jointly optimizing the transmit power of the PB P_{s}, the time of active transmission τ_{a}, the reflection coefficient vector $\boldsymbol{\alpha} = [\alpha_1, \alpha_2, \ldots, \alpha_M]$, the transmit power vector $p = [p_1, p_2, \ldots, p_M]$ and the backscatter time vector $\boldsymbol{\tau}^{\mathrm{b}} = [\tau_1^{\mathrm{b}}, \tau_2^{\mathrm{b}}, \ldots, \tau_M^{\mathrm{b}}]$ of IoT devices. In particular, the throughput maximization problem under the max-min fairness criterion for the considered network can be formulated as

$$P_1: \max_{P_{\mathrm{s}}, \boldsymbol{\tau}^{\mathrm{b}}, \boldsymbol{\alpha}, p, \tau_{\mathrm{a}}} \min_{i \in \mathcal{M}} \quad R_i^{\mathrm{tot}} \tag{7a}$$

$$\text{s.t. C1}: P_{\mathrm{c},i} \tau_i^{\mathrm{b}} + \left(p_i + p_{\mathrm{c},i}\right) \tau_{\mathrm{a}} \leq E_{\mathrm{total}}^{i}, \quad \forall i, \tag{7b}$$

$$\text{C2}: 0 \leq P_{\mathrm{s}} \leq P_{\max}, \tag{7c}$$

$$\text{C3}: \sum_{i=1}^{M} \tau_i^{\mathrm{b}} + \tau_{\mathrm{a}} \leq T, \tag{7d}$$

$$\text{C4}: \ 0 \leq \alpha_i \leq 1, \quad \forall i, \tag{7e}$$

$$\text{C5}: 0 < p_i \leq p_{\max}^{i}, \quad \forall i, \tag{7f}$$

$$\text{C6}: \ \tau_i^{\mathrm{b}} \geq 0, \quad \forall i, \tau_{\mathrm{a}} \geq 0, \tag{7g}$$

where $\mathcal{M} = \{1, 2, \ldots, M\}$ is the set of IoT devices; $P_{\mathrm{c},i}$ and $p_{\mathrm{c},i}$ denote the constant circuit power consumption of the i-th IoT device during the backscatter phase and the uplink NOMA phase, respectively; $P_{\max}$ is the maximum allowed transmit power at the PB; $p_{\max}^{i}$ denotes the maximum transmit power of the i-th IoT device.

In P_1, C1 is the non-overflowing energy constraint for each IoT device within each transmission block, i.e., the total energy consumption at the i-th IoT device should not exceed its harvested energy. C2 and C5 constrain the maximum transmission powers at the PB and the i-th IoT device, respectively. C3 is a constraint of the total time for backscattering and transmitting. C4 constrains the range of α_i and C6 indicates a non-negative parameters for time allocation.

It is obvious that the optimization problem P_1 is highly non-convex due to the following reasons. Firstly, the objective function is very complicated due to the max-min function and the existence of coupling variables, e.g., P_{s}, α_i and τ_i^{b} are coupled in the first term of the objective function. Secondly,

[3]The joint optimization of SIC order and communication resource may further improve the max-min throughput, which can be left for my future work.

constraint C1 is non-convex due to the coupled variables. Therefore, the problem P_1 can not be solved by using existing convex tools. This motivates us to transform this original non-convex problem into a more traceable problem and propose an iterative algorithm to obtain the optimal solutions in the next two subsections.

B. PROBLEM TRANSFORMATION

In order to deal with the max-min function in the objective function, we first introduce a slack variable $\lambda = \min_{i\in\mathcal{M}} R_i^{\text{tot}}$ and transform the original problem P_1 as

$$P_2: \max_{P_{\text{s}},\boldsymbol{\tau}^{\text{b}},\boldsymbol{\alpha},p,\tau_{\text{a}},\lambda} \quad \lambda \tag{8a}$$

$$\text{s.t. C1 - C6,} \tag{8b}$$

$$\text{C7}: R_i^{\text{tot}} \geq \lambda, \quad \forall i. \tag{8c}$$

The problem P_2 is still non-convex due to the non-convex constraints C1 and C7, in which the coupled variables, e.g., P_{s}, α_i, p_i and τ_i^{b}, exist. In order to solve P_2, we provide the following lemma to obtain the optimal transmit power of the PB.

Lemma 1: For the investigated network, the maximum throughput among the IoT device with the max-min fairness criterion is achieved when the PB broadcasts RF signals with the maximum transmit power, that is to say, $P_{\text{s}}^* = P_{\max}$ holds.

Proof. See Appendix A. ■

By substituting $P_{\text{s}}^* = P_{\max}$ into P_2, we have

$$P_3: \max_{\boldsymbol{\tau}^{\text{b}},\boldsymbol{\alpha},p,\tau_{\text{a}},\lambda} \quad \lambda \tag{9a}$$

$$\text{s.t. C1:} P_{\text{c},i}\tau_i^{\text{b}} + \left(p_i + p_{\text{c},i}\right)\tau_{\text{a}} \leq P_{\max}\Big[\eta_i\left(1-\alpha_i\right)h_{\text{P},i}\tau_i^{\text{b}} + \sum_{j=1,j\neq i}^{M}\eta_i\left(h_{\text{P},i} + \alpha_j h_{\text{P},j}h_{j,i}\right)\tau_j^{\text{b}}\Big], \quad \forall i, \tag{9b}$$

$$\text{C3} - \text{C6}, \tag{9c}$$

$$\text{C7}: B\tau_i^{\text{b}}\log_2\left(1 + \frac{\xi\varepsilon_i\alpha_i P_{\max}h_{\text{P},i}h_{i,\text{R}}}{B\sigma^2}\right) + R_i^{\text{a}} \geq \lambda, \quad \forall i, \tag{9d}$$

In order to tackle the coupled relationships between α_i and τ_i^{b} in C1 and C7, and between p_i and τ_{a} in C1, we further introduce a series of auxiliary variables: $x_i = \alpha_i\tau_i^{\text{b}}$ and $P_i = p_i\tau_{\text{a}}$, $i \in \mathcal{M}$. Substituting the above auxiliary variables into P_3, the following problem is reached, i.e.,

$$P_4: \max_{\boldsymbol{\tau}^{\text{b}},x,P,\tau_{\text{a}},\lambda} \quad \lambda \tag{10a}$$

$$\text{s.t. C8:} P_{\text{c},i}\tau_i^{\text{b}} + P_i + p_{\text{c},i}\tau_{\text{a}} \leq P_{\max}\Big[\eta_i\left(\tau_i^{\text{b}} - x_i\right)h_{\text{P},i} + \sum_{j=1,j\neq i}^{M}\eta_i\left(\tau_j^{\text{b}}h_{\text{P},i} + x_j h_{\text{P},j}h_{j,i}\right)\Big], \quad \forall i, \tag{10b}$$

$$\text{C9:} 0 \leq x_i \leq \tau_i^{\text{b}}, \quad \forall i, \tag{10c}$$

$$\text{C10:} 0 < P_i \leq \tau_{\text{a}}p_{\max}^i, \forall i, \tag{10d}$$

$$\text{C3, C6}, \tag{10e}$$

$$\text{C11}: B\tau_i^{\text{b}}\log_2\left(1 + \frac{\xi\varepsilon_i x_i P_{\max}h_{\text{P},i}h_{i,\text{R}}}{\tau_i^{\text{b}}B\sigma^2}\right) + C_i^{\text{a}}\left(\{P_i\}_{i=1}^{M}, \tau_{\text{a}}\right) \geq \lambda, \quad \forall i, \tag{10f}$$

where $x = [x_1, x_2, \ldots, x_M]$, $P = [P_1, P_2, \ldots, P_M]$ and $C_i^{\text{a}}\left(\{P_m\}_{m=i}^{M}, \tau_{\text{a}}\right) = B\tau_{\text{a}}\log_2\left(1 + \frac{P_i h_{i,\text{R}}}{\sum_{m=i+1}^{M}P_m h_{m,\text{R}} + \tau_{\text{a}}B\sigma^2}\right)$. Constraints C8, C9, C10 and C11 are derived form constraints C1, C4, C5 and C7, respectively, by using the introduced auxiliary variables.

For the problem P_4, one observation is that the objective function is linear and all the constraints except C11 are convex constraints. Thus, the convexity of the problem P_4 depends on the constraint C11. However, one can see that the constraint C11 is not convex. This is because the co-channel interference caused by the uplink NOMA makes $C_i^{\text{a}}\left(\{P_m\}_{m=i}^{M}, \tau_{\text{a}}\right)$ jointly non-concave with respect to $\{P_m\}_{m=i}^{M}$ and τ_{a}. In the following part, by means of an inequality, we first considers a relaxation of this non-convex problem P_4, i.e., $C_i^{\text{a}}\left(\{P_m\}_{m=i}^{M}, \tau_{\text{a}}\right)$ is substituted by its low bound, so as to avoid the difference of convex (DC) structure. Then we introduce several auxiliary variables to convert the relaxation problem to a convex problem and obtain the optimal solution to this convex problem by means of the existing convex tools. Finally, we will update the parameters of the used inequality based on the solution obtained in the previous step, and repeat the above two steps until the lower bound becomes tight.

Towards this end, according to [31], Theorem 1 is provided as follows.

Theorem 1: For $\gamma, \tilde{\gamma} > 0$, we have the following inequality: $\log_2(1+\gamma) \geq \omega\log_2(\gamma) + \mu$ with the constant parameters $\omega = \frac{\tilde{\gamma}}{1+\tilde{\gamma}}$ and $\mu = \log_2(1+\tilde{\gamma}) - \omega\log_2(\tilde{\gamma})$, where the lower bound is tight at $\tilde{\gamma} = \gamma$.

Based on Theorem 1, we can obtain the following inequality, i.e.,

$$\begin{aligned} &C_i^{\text{a}}\left(\{P_i\}_{i=1}^{M}, \tau_{\text{a}}\right) \\ &= B\tau_{\text{a}}\log_2\left(1 + \frac{P_i h_{i,\text{R}}}{\sum_{m=i+1}^{M}P_m h_{m,\text{R}} + \tau_{\text{a}}B\sigma^2}\right) \\ &\geq B\tau_{\text{a}}\left[\omega_i\log_2\left(\frac{P_i h_{i,\text{R}}}{\sum_{m=i+1}^{M}P_m h_{m,\text{R}} + \tau_{\text{a}}B\sigma^2}\right) + \mu_i\right], \end{aligned} \tag{11}$$

where ω_i and μ_i are two constants in this iteration of the proposed iterative algorithm and determined by the obtained solution in the pervious iteration. Specifically, let $\left\{\left\{\tau_i^{\text{b}(k)}\right\}_{i=1}^{M}, \left\{P_i^{(k)}\right\}_{i=1}^{M}, \tau_{\text{a}}^{(k)}, \left\{x_i^{(k)}\right\}_{i=1}^{M}, \lambda^{(k)}\right\}$ denote the

obtained solution in the k-th iteration. In the $(k+1)$-th iteration, ω_i and μ_i can be updated as

$$\omega_i = \frac{P_i^{(k)} h_{i,\mathrm{R}}}{\sum_{m=i+1}^{M} P_m^{(k)} h_{m,\mathrm{R}} + \tau_{\mathrm{a}}^{(k)} B\sigma^2 + P_i^{(k)} h_{i,\mathrm{R}}}, \tag{12}$$

$$\mu_i = \log_2\left(1 + \frac{P_i^{(k)} h_{i,\mathrm{R}}}{\sum_{m=i+1}^{M} P_m^{(k)} h_{m,\mathrm{R}} + \tau_{\mathrm{a}}^{(k)} B\sigma^2}\right) - \omega_i \log_2\left(\frac{P_i^{(k)} h_{i,\mathrm{R}}}{\sum_{m=i+1}^{M} P_m^{(k)} h_{m,\mathrm{R}} + \tau_{\mathrm{a}}^{(k)} B\sigma^2}\right). \tag{13}$$

Based on (11), P_4 can be relaxed as

$$P_5: \max_{\boldsymbol{\tau}^{\mathrm{b}}, x, P, \tau_{\mathbf{a}}, \lambda} \lambda \tag{14a}$$

$$\text{s.t. C3,C6,C8,C9,C10,}$$

$$\mathrm{C12}: B\tau_{\mathrm{a}}\left[\omega_i \log_2\left(\frac{P_i h_{i,\mathrm{R}}}{\sum_{m=i+1}^{M} P_m h_{m,\mathrm{R}} + \tau_{\mathrm{a}} B\sigma^2 x}\right) + \mu_i\right] + B\tau_i^{\mathrm{b}} \log_2\left(1 + \frac{\xi \varepsilon_i x_i P_{\max} h_{\mathrm{P},i} h_{i,\mathrm{R}}}{\tau_i^{\mathrm{b}} B\sigma^2}\right) \geq \lambda, \tag{14b}$$

$$\forall i, \tag{14c}$$

where the constraint C12 is transformed from C11.

Although the relaxation P_5 still has non-convex form due to the non-convex constraint C12, the following new auxiliary variables, $y_i = \tau_{\mathrm{a}} \log_2\left(\frac{P_i}{\tau_{\mathrm{a}}}\right)$, $i \in \mathcal{M}$, are introduced to tackle this problem. Thus we have $P_i = \tau_{\mathrm{a}} 2^{\frac{y_i}{\tau_{\mathrm{a}}}}$, $i \in \mathcal{M}$. By replacing P_i with y_i, the constraints C8, C10 and C12 can be rewritten as C13, C14, and C15, respectively, i.e.,

$$\mathrm{C13}: P_{\mathrm{c},i}\tau_i^{\mathrm{b}} + \tau_{\mathrm{a}} 2^{\frac{y_i}{\tau_{\mathrm{a}}}} + p_{\mathrm{c},i}\tau_{\mathrm{a}} \leq P_{\max}\eta_i\left(\tau_i^{\mathrm{b}} - x_i\right) h_{\mathrm{P},i} + P_{\max}\sum_{j=1, j\neq i}^{M} \eta_i\left(\tau_j^{\mathrm{b}} h_{\mathrm{P},i} + x_j h_{\mathrm{P},j} h_{j,i}\right), \quad \forall i; \tag{15}$$

$$\mathrm{C14}: \tau_{\mathrm{a}} 2^{\frac{y_i}{\tau_{\mathrm{a}}}} \leq \tau_{\mathrm{a}} p_{\max}^i, \forall i; \tag{16}$$

$$\mathrm{C15}: B\omega_i y_i + B\tau_{\mathrm{a}}\mu_i + B\omega_i\tau_{\mathrm{a}}\log_2\left(h_{i,\mathrm{R}}\right) - B\omega_i\tau_{\mathrm{a}}\log_2\left(\sum_{m=i+1}^{M} 2^{\frac{y_m}{\tau_{\mathrm{a}}}} h_{m,\mathrm{R}} + B\sigma^2\right) + B\tau_i^{\mathrm{b}}\log_2\left(1 + \frac{\xi\varepsilon_i x_i P_{\max} h_{\mathrm{P},i} h_{i,\mathrm{R}}}{\tau_i^{\mathrm{b}} B\sigma^2}\right) \geq \lambda, \quad \forall i. \tag{17}$$

Based on C13, C14 and C15, P_5 can be reformulated as

$$P_6: \max_{\boldsymbol{\tau}^{\mathrm{b}}, x, y, \tau_{\mathbf{a}}, \lambda} \lambda \tag{18a}$$

$$\text{s.t. C3,C6,C9,C13,C14, C15.} \tag{18b}$$

where $y = [y_1, y_2, \ldots, y_M]$.

Theorem 2: The optimization problem P_6 can be proved to be convex.

Proof: See Appendix B. ■

Although the problem P_6 is convex, it may not be solved by the CVX tool due to existence of $\tau_{\mathrm{a}} 2^{\frac{y_i}{\tau_{\mathrm{a}}}}$ and $B\omega_i\tau_{\mathrm{a}}\log_2\left(\sum_{m=i+1}^{M} 2^{\frac{y_m}{\tau_{\mathrm{a}}}} h_{m,\mathrm{R}} + B\sigma^2\right)$. In order to circumvent this problem, in the next subsection, we employ the Karush-Kuhn-Tucker (KKT) conditions to analyze the problem P_6 and then devise a computationally efficient iterative algorithm to obtain the optimal solution of problem P_6.

C. ITERATIVE ALGORITHM FOR P_6

We first need the partial Lagrangian function for problem P_6, which can be written as (19), shown at the top of the next page. In (19), $\boldsymbol{\theta} = [\theta_1, \theta_2, \ldots, \theta_M] \succeq \mathbf{0}$, $\boldsymbol{\phi} = [\phi_1, \phi_2, \ldots, \phi_M] \succeq \mathbf{0}$, $\boldsymbol{\varpi} = [\varpi_1, \varpi_2, \ldots, \varpi_M] \succeq \mathbf{0}$, and $\boldsymbol{\nu} = [\nu_1, \nu_2, \ldots, \nu_M] \succeq \mathbf{0}$ are the Lagrange multiplier vectors. Since the problem P_6 is convex, the maximization of the partial Lagrangian function $\mathcal{L}$ with respect to the optimization variables $(\boldsymbol{\tau}^{\mathrm{b}}, x, y, \tau_{\mathbf{a}}, \lambda)$ is a standard concave optimization problem for any given Lagrange multiplier vectors $(\boldsymbol{\theta}, \boldsymbol{\phi}, \boldsymbol{\varpi}, \boldsymbol{\nu})$, and the optimal solution can be derived from the KKT conditions [32].

Using the KKT conditions and (19), the following Theorem can be obtained.

$$\mathcal{L} = \lambda + \sum_{i=1}^{M}\theta_i\left(P_{\max}\left(\eta_i\left(\tau_i^{\mathrm{b}} - x_i\right)h_{\mathrm{P},i} + \sum_{j=1, j\neq i}^{M}\eta_i\left(\tau_j^{\mathrm{b}} h_{\mathrm{P},i} + x_j h_{\mathrm{P},j} h_{j,i}\right)\right) - P_{\mathrm{c},i}\tau_i^{\mathrm{b}} - \tau_{\mathrm{a}} 2^{\frac{y_i}{\tau_{\mathrm{a}}}} - p_{\mathrm{c},i}\tau_{\mathrm{a}}\right) + \sum_{i=1}^{M}\phi_i\left(\tau_i^{\mathrm{b}} - x_i\right) + \sum_{i=1}^{M}\varpi_i\left(B\omega_i y_i + B\tau_{\mathrm{a}}\mu_i + B\omega_i\tau_{\mathrm{a}}\log_2\left(h_{i,\mathrm{R}}\right) - B\omega_i\tau_{\mathrm{a}}\log_2\left(\sum_{m=i+1}^{M} 2^{\frac{y_m}{\tau_{\mathrm{a}}}} h_{m,\mathrm{R}} + B\sigma^2\right) + B\tau_i^{\mathrm{b}}\log_2\left(1 + \frac{\xi\varepsilon_i x_i P_{\max} h_{\mathrm{P},i} h_{i,\mathrm{R}}}{\tau_i^{\mathrm{b}} B\sigma^2}\right) - \lambda\right) + \sum_{i=1}^{M}\nu_i\left(\tau_{\mathrm{a}} p_{\max}^i - \tau_{\mathrm{a}} 2^{\frac{y_i}{\tau_{\mathrm{a}}}}\right) \tag{19}$$

Algorithm 1 Iterative Algorithm for Solving P_6

1: Initialize $\boldsymbol{\theta}$, $\boldsymbol{\phi}$, $\boldsymbol{\varpi}$, and $\boldsymbol{\nu}$;
2: **repeat**
3: Obtain the optimal transmit power vectors $\{p_i^*\}_{i=1}^M$ and reflection coefficient vectors $\{\alpha_i^*\}_{i=1}^M$ at IoT devices based on (25) and (26);
4: Obtain $\{\tau_i^{\mathrm{b}*}\}_{i=1}^M$, τ_{a}^* and λ^* by solving the optimization problem P_7 with given $\boldsymbol{\theta}$, $\boldsymbol{\phi}$, $\boldsymbol{\varpi}$, and $\boldsymbol{\nu}$;
5: Update $\boldsymbol{\theta}$, $\boldsymbol{\phi}$, $\boldsymbol{\varpi}$, and $\boldsymbol{\nu}$ by using the gradient method;
6: **until** $\boldsymbol{\theta}$, $\boldsymbol{\phi}$, $\boldsymbol{\varpi}$, and $\boldsymbol{\nu}$ converge;
7: Output the optimal solutions to P_6.

Theorem 3: For any given Lagrange multiplier vectors, we can derive the closed-form expressions of the optimal transmit power and the optimal reflection coefficient for the i-th IoT device, given by

$$p_i^* = \frac{P_i^*}{\tau_{\mathrm{a}}^*} = 2^{\frac{y_i^*}{\tau_{\mathrm{a}}^*}} = \left[\frac{B\varpi_i\omega_i}{(\theta_i+\nu_i)\ln 2}\right]^+, \tag{20}$$

$$\alpha_i^* = \frac{x_i^*}{\tau_i^{\mathrm{b}*}} = \left[\frac{\varpi_i B}{\left(\phi_i+\theta_i P_{\max}\eta_i h_{\mathrm{P},i}\right)\ln 2} - \frac{B\sigma^2}{\xi\varepsilon_i P_{\max} h_{\mathrm{P},i} h_{i,\mathrm{R}}}\right]^+, \tag{21}$$

where $[x]^+ = \max\{0, x\}$. Besides, the Lagrangian function $\mathcal{L}$ is a linear function with respect to τ_{a}, τ_i^{b} and λ.

Proof: See Appendix C. ■

Remark 1: Eq. (20) reveals that when $p_i^* > 0$, the i-th IoT device will exhaust all the harvested energy or use the maximum transmit power for uplink NOMA. The reasons are as follows. $p_i^* > 0$ yields $\theta_i + \nu_i > 0$, resulting in $\theta_i > 0$ or $\nu_i > 0$. Combining the complementary slackness conditions $\theta_i\left(P_{\max}\left(\eta_i\left(\tau_i^{\mathrm{b}} - x_i\right)h_{\mathrm{P},i} + \sum_{j=1,j\neq i}^{M}\eta_i\left(\tau_j^{\mathrm{b}}h_{\mathrm{P},i} + x_j h_{\mathrm{P},j}h_{j,i}\right)\right) - P_{\mathrm{c},i}\tau_i^{\mathrm{b}} - \tau_{\mathrm{a}}2^{\frac{y_i}{\tau_{\mathrm{a}}}} - p_{\mathrm{c},i}\tau_{\mathrm{a}}\right) = 0$ and $\nu_i\left(\tau_{\mathrm{a}}p_{\max}^i - \tau_{\mathrm{a}}2^{\frac{y_i}{\tau_{\mathrm{a}}}}\right) = 0$, we can draw the above conclusions.

Remark 2: Eq. (21) shows that with the increase of $P_{\max}$, α_i^* should be reduced for maximizing the minimal throughout of each IoT device. This indicates that when the received power at the IoT device increases, in order to achieve the max-min throughput, the IoT devices prefer to split more power for EH and the harvested energy will be used in the uplink NOMA phase. This is because the uplink NOMA, one of active transmission modes, achieves a higher throughput than the passive BackCom.

As pointed out by Theorem 3, the Lagrangian function $\mathcal{L}$ is a linear function with respect to τ_{a}, τ_i^{b} and λ. This means that the optimal backscatter time $\tau_i^{\mathrm{b}*}$, the optimal time of active transmission τ_{a}^* and the optimal max-min throughput λ^* can be obtained at the vertices of the feasible region [32]. In order to obtain $\tau_i^{\mathrm{b}*}$, τ_{a}^* and λ^*, after substituting (20) and (21) into P_5, we can obtain the following optimization problem, given as

$$P_7: \max_{\boldsymbol{\tau}^{\mathrm{b}},\tau_{\mathrm{a}},\lambda} \lambda \tag{22a}$$

$$\text{s.t. C16: } P_{\mathrm{c},i}\tau_i^{\mathrm{b}} + \tau_{\mathrm{a}}p_i^* + p_{\mathrm{c},i}\tau_{\mathrm{a}} \leq P_{\max}\left[\eta_i\left(\tau_i^{\mathrm{b}} - \tau_i^{\mathrm{b}}\alpha_i^*\right)h_{\mathrm{P},i} + \sum_{j=1,j\neq i}^{M}\eta_i\left(\tau_j^{\mathrm{b}}h_{\mathrm{P},i} + \tau_j^{\mathrm{b}}\alpha_j^* h_{\mathrm{P},j}h_{j,i}\right)\right], \forall i, \tag{22b}$$

$$\text{C3, C6,} \tag{22c}$$

$$\text{C17: } B\tau_{\mathrm{a}}\mu_i + B\omega_i\tau_{\mathrm{a}}\log_2\left(p_i^* h_{i,\mathrm{R}}\right) - B\omega_i\tau_{\mathrm{a}}\log_2\Big(\sum_{m=i+1}^{M}p_m^* h_{m,\mathrm{R}} + B\sigma^2\Big) + B\tau_i^{\mathrm{b}}\log_2\Big(1 + \frac{\xi\varepsilon_i\alpha_i^* P_{\max}h_{\mathrm{P},i}h_{i,\mathrm{R}}}{B\sigma^2}\Big) \geq \lambda, \quad \forall i, \tag{22d}$$

where constraints C16 and C17 are transformed from constraints C13 and C15. It is obvious that the problem P_7 is a linear programming problem of τ_{a}, τ_i^{b} and λ. Thus, standard linear optimization tools [32] can be used to obtain $\tau_i^{\mathrm{b}*}$, τ_{a}^* and λ^*. Accordingly, the process of how to obtain the optimal solutions to P_6 is shown in Algorithm 1. Please note that here gradient method is used to update the Lagrange multipliers [32] and the details are omitted here for convenience.

D. TWO-LAYER ITERATIVE ALGORITHM FOR P_1

Based on Section III-B and Section III-C, we can propose a two-layer iterative algorithm to solve the original optimization problem P_1, given by Algorithm 2, in which in the inner loop, we aim to solve the problem P_6 by means of Algorithm 1, and in the outer loop, we should update the values of ω_i and μ_i, $\forall i$ until the stop condition is satisfied. In particular, in the k-th iteration, we use Algorithm 1 to solve P_6 with ω_i^k and μ_i^k, $\forall i$, and obtain the optimal solutions to P_6, which can be denoted by $\{x_i^+\}_{i=1}^M$, $\{\tau_i^{\mathrm{b}+}\}_{i=1}^M$, τ_{a}^+, $\{y_i^+\}_{i=1}^M$ and λ^+. On this basis, we can obtain the optimal transmit power vectors $\{p_i^+\}_{i=1}^M$ and reflection coefficient vectors $\{\alpha_i^+\}_{i=1}^M$ at IoT devices, and update $\lambda_k = \lambda^+$. Given an error tolerance ε, if the stop condition, $|\lambda_k - \lambda_{k-1}| < \varepsilon$, is satisfied, the obtained solution $\{\{\alpha_i^+\}_{i=1}^M, \{\tau_i^{\mathrm{b}+}\}_{i=1}^M, \tau_{\mathrm{a}}^+, \{p_i^+\}_{i=1}^M\}$ is the optimal solution to P_1 and the obtained max-min throughput is given by λ^+. Otherwise, let $k = k+1$ and update ω_i^k and μ_i^k, $\forall i$ based on the obtained solution $\{\{\alpha_i^+\}_{i=1}^M, \{\tau_i^{\mathrm{b}+}\}_{i=1}^M, \tau_{\mathrm{a}}^+, \{p_i^+\}_{i=1}^M\}$ by following (12) and (13).

Note that the iteration to update α_k and μ_k always converges and the equality in (11) holds at the converged solution. The detailed proof can be refer to [31].

It is worth noting that the proposed iterative algorithm mentioned in this work is Algorithm 2 which can be used to solve the problem P_1, while Algorithm 1 is adopted in each iteration of Algorithm 2 to solve P_6. The proposed iterative algorithm can be adopted to obtain the proposed resource allocation scheme for IoT networks with a massive number

Algorithm 2 Two-Layer Iterative Algorithm

Set the maximum tolerance ε;
Set the iteration index $k = 1$, Flag $= 1$ and $\lambda_0 = 0$;
Set $\omega_i^k = 1$, $\mu_i^k = 0$ for $i \in \mathcal{M}$;
repeat
  Solve the optimization problem P_6 with given ω_i^k and μ_i^k, $\forall i$, to obtain the optimal solutions, denoted by $\{x_i^+\}_{i=1}^M$, $\{\tau_i^{\mathrm{b}+}\}_{i=1}^M$, τ_{a}^+,$\{y_i^+\}_{i=1}^M$ and λ^+, by means of Algorithm 1;
  Obtain the optimal transmit power vectors $\{p_i^+\}_{i=1}^M$ and reflection coefficient vectors $\{\alpha_i^+\}_{i=1}^M$ at IoT devices based on the obtained $\{x_i^+\}_{i=1}^M$, $\{\tau_i^{\mathrm{b}+}\}_{i=1}^M$, τ_{a}^+ and $\{y_i^+\}_{i=1}^M$;
  Obtain the optimal transmit power of the PB as $P_{\mathrm{s}}^+ = P_{\max}$ and set $\lambda_k = \lambda^+$;
  if $|\lambda_k - \lambda_{k-1}| \geq \varepsilon$ **then**
    Set $k = k + 1$;
    Update ω_i^k and μ_i^k, $\forall i$, based on (12) and (13);
  else
    The obtained solution $\{\{\alpha_i^+\}_{i=1}^M, \{\tau_i^{\mathrm{b}+}\}_{i=1}^M, \tau_{\mathrm{a}}^+, \{p_i^+\}_{i=1}^M\}$ is the optimal solution to P_1 and the obtained max-min throughput is given by λ^+;
    Set Flag $= 0$;
  end if
until Flag $= 0$;
Output the max-min throughput of IoT devices and the optimal solution.

of IoT devices and its computational complexity will also increase with the increasing of M. Specifically, the computational complexity of the proposed iterative algorithm can be evaluated as follows. According to [32], [33], τ_{a}, λ, p_i, α_i and τ_i^{b}, $\forall i$, have a linear computational complexity with the number of IoT devices, M, and the computational complexity for updating Lagrange variables is given by $O(M^2)$, where $O(x)$ denotes the upper bound for the computational complexity grows with order x. Since the computational complexity for updating auxiliary variables ω_i and μ_i, $\forall i$ is independent of M, the total computational complexity for solving P_1 is given by $O(M^3)$.

IV. SIMULATIONS

In this section, we verify the effectiveness and the superiority of the proposed scheme under the considered network by means of computer simulations. Unless otherwise specified, the basic simulation parameters are set as follows. Following [25], [26], we set $M = 4$, $T = 1$s, $W = 100$kHz, $\sigma^2 = -120$dBm/Hz, $\xi = -15$dB, $P_{\mathrm{c},1}^b = P_{\mathrm{c},2}^b = P_{\mathrm{c},3}^b = P_{\mathrm{c},4}^b = 10\mu$W, $p_{\mathrm{c},1} = p_{\mathrm{c},2} = p_{\mathrm{c},3} = p_{\mathrm{c},4} = 1$mW and $P_{\max} = 3$W. The energy conversion efficiency is set as $\eta_1 = \eta_2 = \eta_3 = \eta_4 = 0.7$. The standard power loss propagation model is considered for modelling the channel gains among the PB, the IR and multiple IoT devices. Specifically, let $g_{\mathrm{P},i}$, $g_{i,j}$, and $g_{i,\mathrm{R}}$ denote the small-scale fading of the PB-to-the i-th IoT device link, the i-th IoT device-to-the j-th IoT device link and the i-th IoT device-to-IR link, respectively, where $i, j = 1, 2, \ldots, M$ and $i \neq j$. Denote the distances of the PB-to-the i-th IoT device link, the i-th IoT device-to-the j-th IoT device link and the i-th IoT device-to-IR link as $d_{\mathrm{P},i}$, $d_{i,j}$, and $d_{i,\mathrm{R}}$, respectively. Then we have $h_{\mathrm{P},i} = g_{\mathrm{P},i} d_{\mathrm{P},i}^{-\beta}$, $h_{i,j} = g_{i,j} d_{i,j}^{-\beta}$ and $h_{i,\mathrm{R}} = g_{i,\mathrm{R}} d_{i,\mathrm{R}}^{-\beta}$, where β is the path loss exponent. Here we set $\beta = 3$. According to [33], we assume that four IoT devices are randomly and uniformly distributed on every side of the PB with a reference distance of 2 meters and a maximum service distance of 10 meters. Similarly, the distance between different IoT devices also varies from 2 meters to 10 meters. The distances from the IoT devices to the IR are set as: $d_{1,\mathrm{R}} = 55$ meters, $d_{2,\mathrm{R}} = 60$ meters, $d_{3,\mathrm{R}} = 63$ meters and $d_{4,\mathrm{R}} = 67$ meters.

Fig. 2 illustrates the convergence of the proposed algorithm under different sets of $P_{\max}$ and ξ. Specifically, Fig. 2(a)

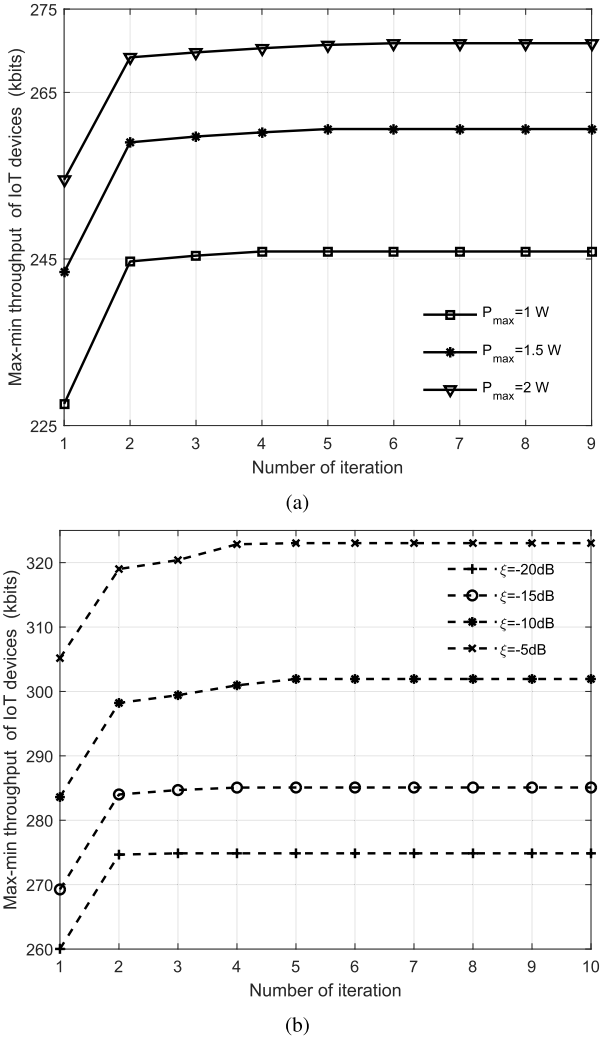

FIGURE 2. The convergence of the proposed algorithm under different sets of $P_{\max}$ and ξ.

shows the max-min throughput of IoT devices versus the number of iterations under different settings of $P_{\max}$ while Fig. 2(b) plots the convergence of the proposed algorithm under different sets of ξ. It can be seen that the proposed algorithm can always converge to a stable throughput after the limited iterations. For example, when $P_{\max} = 2$W, about 7 iterations can ensure the convergence of the proposed scheme. This demonstrates that our proposed iterative algorithm is computationally efficient.

Fig. 3 shows the max-min throughput of IoT devices versus the performance gap ξ under three schemes, which are the proposed scheme, wireless powered BackCom and wireless powered NOMA, respectively. For wireless powered BackCom, we set $\tau_a = 0$ and $p_i = 0, \forall i$, while for wireless powered NOMA, we set $\alpha_i = 0, \forall i$. Note that wireless powered BackCom and wireless powered NOMA are optimized under the same constraints as P_1. As shown in this figure, we can observe that with the increasing of ξ, the max-min throughput of the IoT devices under the proposed scheme and wireless powered BackCom will increase while the throughput under wireless powered NOMA will keep unchanged. This is because the throughput achieved by BackCom will increase as ξ increases while the throughput under wireless powered NOMA is not influenced by ξ. By comparisons, we can also see that the proposed scheme can achieve the highest max-min throughput among the three schemes, as the proposed scheme provides more flexibility to utilize the resource efficiently to maximize the minimum throughput of IoT devices and both wireless powered BackCom and wireless powered NOMA can be regarded as special cases for the proposed scheme. This also indicates the rational of considering the combination of BackCom and wireless powered NOMA in this work.

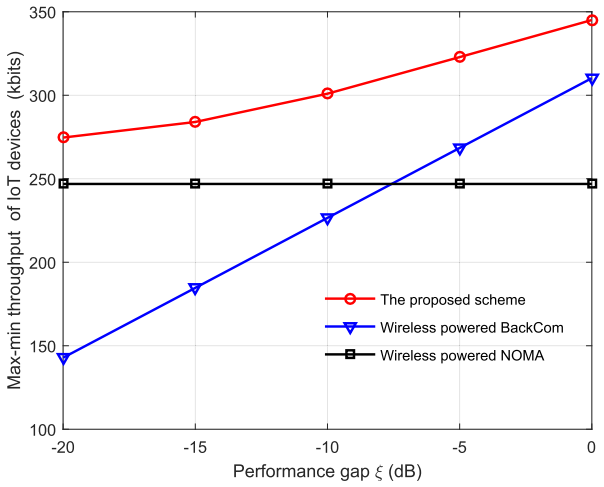

FIGURE 3. Throughput versus the performance gap ξ.

Fig. 4 shows the max-min throughput achieved by IoT devices versus the maximum transmit power of the PB $P_{\max}$. In order to illustrate the superiority of the proposed scheme, we compare the max-min throughput achieved by the proposed scheme with that under wireless powered BackCom, wireless powered NOMA and hybrid of wireless powered OMA and BackCom. It is worth noting that for hybrid of wireless powered OMA and BackCom, M IoT devices adopt a TDMA scheme instead of uplink NOMA to transmit information to the IR and the max-min throughput for hybrid of wireless powered OMA and BackCom is optimized under the same constraints as P_1, which has been studied in [25]. As shown in this figure, we can see that the max-min throughput under the proposed scheme, wireless powered BackCom, wireless powered NOMA and hybrid of wireless powered OMA and BackCom will increase as $P_{\max}$ increases. This is because the optimal transmit power of the PB is given by $P_{\max}$ and the max-min throughput increases with the increasing of the optimal transmit power of the PB. By comparisons, we can also observe that the proposed scheme can achieve the highest max-min throughput. This also demonstrates the necessary and importance of considering NOMA for uplink transmission.

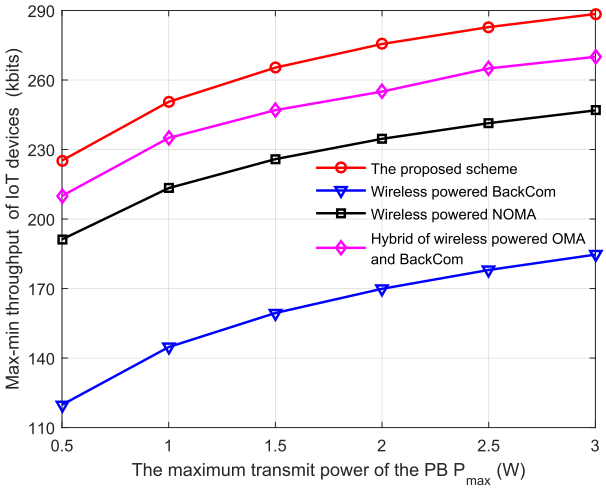

FIGURE 4. Throughput versus the maximum transmit power of the PB $P_{\max}$.

Fig. 5 compares the fairness among different IoT devices achieved by the proposed scheme under the max-min fairness criterion with the existing scheme achieved by the sum throughput maximization. It is worth noting that the scheme under the sum throughput maximization is to maximize the sum of throughput of all the IoT devices under the same constraints as P_1. After obtaining the optimal resource allocation for maximizing the minimum throughput of IoT devices or the sum throughput of IoT devices, we can compute the throughput of each IoT device and the average throughput that can be determined by $\frac{\sum_{i=1}^{M} \text{Throughput of the } i\text{-th IoT device}}{M}$. We consider two scenarios, where one is the scenario with a small channel gain difference and the other is the scenario with a large channel gain difference. By comparisons, we can observe that the proposed scheme can greatly improve the fairness among different IoT devices at the cost of a small reduction to

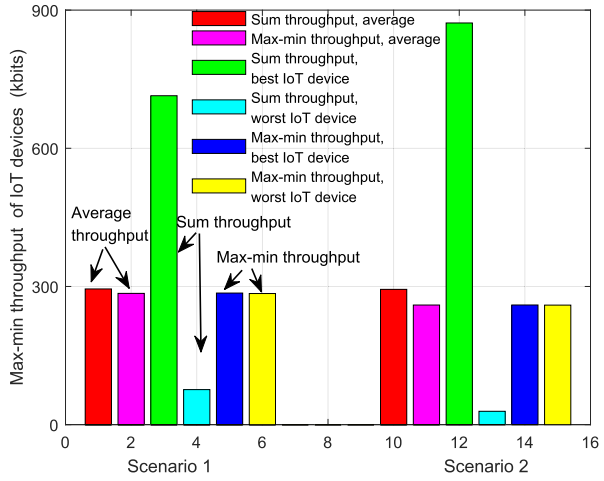

FIGURE 5. Fairness comparison under different schemes.

the average throughput. Besides, we can also see that the proposed scheme is more effective in terms of fairness among different IoT devices for the case with a larger channel gain difference.

V. CONCLUSION

In this work, we have proposed a novel backscatter assisted wireless powered NOMA network, where each IoT device can backscatter its information via BackCom and transmit its information via uplink NOMA to the IR. In order to ensure throughput fairness among IoT devices, we have formulated a throughput maximization problem under the max-min fairness criterion by jointly optimizing the transmit power of the PB, the backscatter time, reflection coefficients, and transmit power of IoT devices as well as the time for uplink NOMA. A two-layer iterative algorithm has been proposed to obtain the optimal solution. Simulation results have shown the quick convergence of the proposed algorithm, and demonstrated the superiority of the proposed scheme in terms of the max-min throughput achieved by IoT devices by comparing with existing schemes.

APPENDIX A
PROOF OF THE LEMMA 1

Here we prove Lemma 1 by contradiction. Assume that $\left(P_{\mathrm{s}}^{*}, (\boldsymbol{\tau}^{\mathrm{b}})^{*}, \boldsymbol{\alpha}^{*}, (p)^{*}, \tau_{\mathrm{a}}^{*}\right)$ is the optimal solution to the problem P_2 and satisfying $P_{\mathrm{s}}^{*} < P_{\max}$. Substituting the optimal solution into (6), we can obtain $R_i^{\mathrm{tot}*}$ for a given i, and the max-min throughput can be determined by the following equality, i.e., $\lambda^{*} = \min\left\{R_i^{\mathrm{tot}*}, i \in \mathcal{M}\right\}$. Let's construct another solution $\left(P_{\mathrm{s}}^{+}, (\boldsymbol{\tau}^{\mathrm{b}})^{+}, \boldsymbol{\alpha}^{+}, (p)^{+}, \tau_{\mathrm{a}}^{+}\right)$ satisfying $P_{\mathrm{s}}^{+} = P_{\max} > P_{\mathrm{s}}^{*}$, $(\boldsymbol{\tau}^{\mathrm{b}})^{+} = (\boldsymbol{\tau}^{\mathrm{b}})^{*}$, $\boldsymbol{\alpha}^{+} = \boldsymbol{\alpha}^{*}$, $(p)^{+} = (p)^{*}$, and $\tau_{\mathrm{a}}^{+} = \tau_{\mathrm{a}}^{*}$. Similarly, substituting the solution $\left(P_{\mathrm{s}}^{+}, (\boldsymbol{\tau}^{\mathrm{b}})^{+}, \boldsymbol{\alpha}^{+}, (p)^{+}, \tau_{\mathrm{a}}^{+}\right)$ into (6), $R_i^{\mathrm{tot}+}$ can be determined. Since the throughput achieved by the i-th IoT device, R_i^{tot}, is an increasing function with respect to P_{s}. Thus, $P_{\mathrm{s}}^{+} > P_{\mathrm{s}}^{*}$ results in $R_i^{\mathrm{tot}+} > R_i^{\mathrm{tot}*}$ for any given i. Combining this observation with $\lambda = \min\left\{R_i^{\mathrm{tot}}, i \in \mathcal{M}\right\}$, we have $\lambda^{+} > \lambda^{*}$. This indicates that $\left(P_{\mathrm{s}}^{*}, (\boldsymbol{\tau}^{\mathrm{b}})^{*}, \boldsymbol{\alpha}^{*}, (p)^{*}, \tau_{\mathrm{a}}^{*}\right)$ is not the optimal solution and hence the $P_{\mathrm{s}}^{*} < P_{\max}$ does not hold. In other words, $P_{\mathrm{s}}^{*} = P_{\max}$ should be satisfied for obtaining the max-min throughput in our considered network.

APPENDIX B
PROOF OF THE THEOREM 2

The objective function and the constraints C3, C9, and C6 are linear, thus in what follows, we only need to prove that the constraints C13, C14, and C15 are convex.

On the convexity of C13: One observation from this constraint is that except the term $\tau_{\mathrm{a}} 2^{\frac{y_i}{\tau_{\mathrm{a}}}}$, others are linear. This indicates that C13 is convex if and only if $\tau_{\mathrm{a}} 2^{\frac{y_i}{\tau_{\mathrm{a}}}}$ is a joint convex function with respect to the optimization variables y_i and τ_{a}. Since the perspective function can preserve convexity [32], we know that the convexity of $\tau_{\mathrm{a}} 2^{\frac{y_i}{\tau_{\mathrm{a}}}}$ is the same as that of 2^{y_i}. It is not hard to verify that the 2^{y_i} is a convex function and hence the constraint C13 is convex.

On the convexity of C14: Since in the preceding paragraph, it has been proven that $\tau_{\mathrm{a}} 2^{\frac{y_i}{\tau_{\mathrm{a}}}}$ is a joint convex function, we can conclude that the constraint C14 is convex.

On the convexity of C15: By observing (17), it is not hard to know that the convexity of C15 depends on the two terms: $-B\omega_i\tau_{\mathrm{a}}\log_2\left(\sum_{m=i+1}^{M} 2^{\frac{y_m}{\tau_{\mathrm{a}}}} h_{m,\mathrm{R}} + B\sigma^2\right)$ and $B\tau_i^{\mathrm{b}}\log_2\left(1 + \frac{\xi\varepsilon_i x_i P_{\max} h_{\mathrm{P},i} h_{i,\mathrm{R}}}{\tau_i^{\mathrm{b}} B\sigma^2}\right)$. Similarly, using the perspective function, it can be known that the convexities of $-B\omega_i\tau_{\mathrm{a}}\log_2\left(\sum_{m=i+1}^{M} 2^{\frac{y_m}{\tau_{\mathrm{a}}}} h_{m,\mathrm{R}} + B\sigma^2\right)$ and $B\tau_i^{\mathrm{b}}\log_2\left(1 + \frac{\xi\varepsilon_i x_i P_{\max} h_{\mathrm{P},i} h_{i,\mathrm{R}}}{\tau_i^{\mathrm{b}} B\sigma^2}\right)$ are the same as that of $-B\omega_i\log_2\left(\sum_{m=i+1}^{M} 2^{y_m} h_{m,\mathrm{R}} + B\sigma^2\right)$ and $B\log_2\left(1 + \frac{1}{B\sigma^2} \times \xi\varepsilon_i x_i P_{\max} h_{\mathrm{P},i} h_{i,\mathrm{R}}\right)$, respectively. Combining this observation with the fact the log-sum-exp function is convex and log function is concave, we can conclude that the constraint C15 is convex. Therefore, the optimization problem P_6 is convex.

APPENDIX C
PROOF OF THE THEOREM 3

Taking the partial derivative of $\mathcal{L}$ over all the optimization variables, respectively, we have

$$\frac{\partial \mathcal{L}}{\partial y_i} = -(\theta_i + \nu_i)\left(2^{\frac{y_i}{\tau_{\mathrm{a}}}} \ln 2\right) + B\varpi_i\omega_i, \tag{23}$$

$$\frac{\partial \mathcal{L}}{\partial x_i} = \frac{\varpi_i B\xi\varepsilon_i P_{\max} h_{\mathrm{P},i} h_{i,\mathrm{R}}}{B\sigma^2 + \xi\varepsilon_i P_{\max} h_{\mathrm{P},i} h_{i,\mathrm{R}} \frac{x_i}{\tau_i^{\mathrm{b}}}} \frac{1}{\ln 2} - \phi_i \tag{24}$$

$$-\theta_i P_{\max}\eta_i h_{\mathrm{P},i}, \tag{25}$$

$$\frac{\partial \mathcal{L}}{\partial \tau_{\mathrm{a}}} = \sum_{i=1}^{M} \theta_i \left(\frac{y_i}{\tau_{\mathrm{a}}} 2^{\frac{y_i}{\tau_{\mathrm{a}}}} \ln 2 - 2^{\frac{y_i}{\tau_{\mathrm{a}}}} - p_{c,i}\right)$$

$$+\sum_{i=1}^{M}\varpi_i\left(B\mu_i+B\omega_i\log_2\left(h_{i,\mathrm{R}}\right)\right)$$
$$-\sum_{i=1}^{M}\varpi_i\left(B\omega_i\log_2\left(\sum_{m=i+1}^{M}2^{\frac{y_m}{\tau_\mathrm{a}}}h_{m,\mathrm{R}}+B\sigma^2\right)\right)$$
$$+\sum_{i=1}^{M}\frac{\varpi_i B\omega_i\sum\limits_{m=i+1}^{M}2^{\frac{y_m}{\tau_\mathrm{a}}}\frac{y_m h_{m,\mathrm{R}}}{\tau_\mathrm{a}}}{\sum\limits_{m=i+1}^{M}2^{\frac{y_m}{\tau_\mathrm{a}}}h_{m,\mathrm{R}}+B\sigma^2}$$
$$+\sum_{i=1}^{M}\nu_i\left(p_{\max}^{i}-2^{\frac{y_i}{\tau_\mathrm{a}}}+\frac{y_i}{\tau_\mathrm{a}}2^{\frac{y_i}{\tau_\mathrm{a}}}\ln 2\right), \tag{26}$$

$$\frac{\partial\mathcal{L}}{\partial\tau_i^{\mathrm{b}}}=\theta_i\left(P_{\max}\eta_i h_{\mathrm{P},i}-P_{\mathrm{c},i}\right)+\phi_i$$
$$+\varpi_i B\log_2\left(1+\frac{\xi\varepsilon_i x_i P_{\max}h_{\mathrm{P},i}h_{i,\mathrm{R}}}{\tau_i^{\mathrm{b}}B\sigma^2}\right)$$
$$-\frac{\varpi_i B\xi\varepsilon_i P_{\max}h_{\mathrm{P},i}h_{i,\mathrm{R}}}{\ln 2\left(B\sigma^2+\xi\varepsilon_i P_{\max}h_{\mathrm{P},i}h_{i,\mathrm{R}}\frac{x_i}{\tau_i^{\mathrm{b}}}\right)}\frac{x_i}{\tau_i^{\mathrm{b}}}, \tag{27}$$

$$\frac{\partial\mathcal{L}}{\partial\lambda}=1-\sum_{i=1}^{M}\varpi_i. \tag{28}$$

Setting $\frac{\partial\mathcal{L}}{\partial y_i}=0$ and $\frac{\partial\mathcal{L}}{\partial x_i}=0$, respectively, the optimal transmit power and the optimal reflection coefficient for the i-th IoT device can be derived, given by

$$p_i^*=\frac{P_i^*}{\tau_\mathrm{a}^*}=2^{\frac{y_i^*}{\tau_\mathrm{a}^*}}=\left[\frac{B\varpi_i\omega_i}{(\theta_i+\nu_i)\ln 2}\right]^+. \tag{29}$$

$$\alpha_i^*=\frac{x_i^*}{\tau_i^{\mathrm{b}*}}$$
$$=\left[\frac{\varpi_i B}{\left(\phi_i+\theta_i P_{\max}\eta_i h_{\mathrm{P},i}\right)\ln 2}-\frac{B\sigma^2}{\xi\varepsilon_i P_{\max}h_{\mathrm{P},i}h_{i,\mathrm{R}}}\right]^+. \tag{30}$$

where $[x]^+=\max\{0,x\}$.

Substituting (29) and (30) into (25) and (26), we can rewrite the expressions of $\frac{\partial\mathcal{L}}{\partial\tau_\mathrm{a}}$ and $\frac{\partial\mathcal{L}}{\partial\tau_i^{\mathrm{b}}}$, i.e.,

$$\frac{\partial\mathcal{L}}{\partial\tau_\mathrm{a}}=\sum_{i=1}^{M}\theta_i\left(p_i^*\left(\log_2 p_i^*\right)\ln 2-p_i^*-p_{c,i}\right)$$
$$+\sum_{i=1}^{M}\varpi_i\left(B\mu_i+B\omega_i\log_2\left(h_{i,\mathrm{R}}\right)\right)$$
$$-\sum_{i=1}^{M}\varpi_i\left(B\omega_i\log_2\left(\sum_{m=i+1}^{M}p_m^*h_{m,\mathrm{R}}+B\sigma^2\right)\right)$$
$$+\sum_{i=1}^{M}\frac{\varpi_i B\omega_i\sum\limits_{m=i+1}^{M}p_m^*h_{m,\mathrm{R}}\log_2 p_m^*}{\sum\limits_{m=i+1}^{M}p_m^*h_{m,\mathrm{R}}+B\sigma^2}$$
$$+\sum_{i=1}^{M}\nu_i\left(p_{\max}^{i}-p_i^*+p_i^*\left(\log_2 p_i^*\right)\ln 2\right) \tag{31}$$

$$\frac{\partial\mathcal{L}}{\partial\tau_i^{\mathrm{b}}}=\theta_i\left(P_{\max}\eta_i h_{\mathrm{P},i}-P_{\mathrm{c},i}\right)+\phi_i$$
$$+\varpi_i B\log_2\left(1+\frac{\alpha_i^*\xi\varepsilon_i P_{\max}h_{\mathrm{P},i}h_{i,\mathrm{R}}}{B\sigma^2}\right)$$
$$-\frac{\varpi_i B\xi\varepsilon_i P_{\max}h_{\mathrm{P},i}h_{i,\mathrm{R}}\alpha_i^*}{\ln 2\left(B\sigma^2+\xi\varepsilon_i P_{\max}h_{\mathrm{P},i}h_{i,\mathrm{R}}\alpha_i^*\right)}. \tag{32}$$

Combining eqs. (28), (31), and (32), it is easy to know that Lagrangian function $\mathcal{L}$ is a linear function with respect to τ_a, τ_i^{b} and λ.

REFERENCES

[1] A. Al-Fuqaha, M. Guizani, M. Mohammadi, M. Aledhari, and M. Ayyash, "Internet of Things: A survey on enabling technologies, protocols, and applications," *IEEE Commun. Surveys Tuts.*, vol. 17, no. 4, pp. 2347–2376, 4th Quart., 2015.

[2] B. Clerckx, R. Zhang, R. Schober, D. W. K. Ng, D. I. Kim, and H. V. Poor, "Fundamentals of wireless information and power transfer: From RF energy harvester models to signal and system designs," *IEEE J. Sel. Areas Commun.*, vol. 37, no. 1, pp. 4–33, Jan. 2019.

[3] X. Lu, D. Niyato, H. Jiang, D. I. Kim, Y. Xiao, and Z. Han, "Ambient backscatter assisted wireless powered communications," *IEEE Wireless Commun.*, vol. 25, no. 2, pp. 170–177, Apr. 2018.

[4] F. Rezaei, C. Tellambura, and S. Herath, "Large-scale wireless-powered networks with backscatter communications—A comprehensive survey," *IEEE Open J. Commun. Soc.*, vol. 1, pp. 1100–1130, 2020.

[5] Y. Ye, L. Shi, X. Chu, H. Zhang, and G. Lu, "On the outage performance of SWIPT-based three-step two-way DF relay networks," *IEEE Trans. Veh. Technol.*, vol. 68, no. 3, pp. 3016–3021, Mar. 2019.

[6] S. Bi, Y. Zeng, and R. Zhang, "Wireless powered communication networks: An overview," *IEEE Wireless Commun.*, vol. 23, no. 2, pp. 10–18, Apr. 2016.

[7] L. Shi, L. Zhao, and K. Liang, "Power allocation for wireless powered MIMO transmissions with non-linear RF energy conversion models," *China Commun.*, vol. 14, no. 2, pp. 57–64, Feb. 2017.

[8] S. Bi, C. K. Ho, and R. Zhang, "Wireless powered communication: Opportunities and challenges," *IEEE Commun. Mag.*, vol. 53, no. 4, pp. 117–125, Apr. 2015.

[9] H. Ju and R. Zhang, "Throughput maximization in wireless powered communication networks," *IEEE Trans. Wireless Commun.*, vol. 13, no. 1, pp. 418–428, Jan. 2014.

[10] D. Li, "Capacity of backscatter communication with frequency shift in Rician fading channels," *IEEE Wireless Commun. Lett.*, vol. 8, no. 6, pp. 1639–1643, Dec. 2019.

[11] Y. Ye, L. Shi, R. Qingyang Hu, and G. Lu, "Energy-efficient resource allocation for wirelessly powered backscatter communications," *IEEE Commun. Lett.*, vol. 23, no. 8, pp. 1418–1422, Aug. 2019.

[12] C. Boyer and S. Roy, "Backscatter communication and RFID: Coding, energy, and MIMO analysis," *IEEE Trans. Commun.*, vol. 62, no. 3, pp. 770–785, Mar. 2014.

[13] Y. Ye, L. Shi, X. Chu, and G. Lu, "On the outage performance of ambient backscatter communications," *IEEE Internet Things J.*, vol. 7, no. 8, pp. 7265–7278, Aug. 2020.

[14] D. Li and Y.-C. Liang, "Price-based bandwidth allocation for backscatter communication with bandwidth constraints," *IEEE Trans. Wireless Commun.*, vol. 18, no. 11, pp. 5170–5180, Nov. 2019.

[15] Z. Ling, F. Hu, and D. Li, "Optimal resource allocation in point-to-point wireless body area network with backscatter communication," in *Proc. Int. Conf. Comput., Netw. Commun. (ICNC)*, Feb. 2020, pp. 780–784.

[16] D. T. Hoang, D. Niyato, P. Wang, D. I. Kim, and Z. Han, "Ambient backscatter: A new approach to improve network performance for RF-powered cognitive radio networks," *IEEE Trans. Commun.*, vol. 65, no. 9, pp. 3659–3674, Sep. 2017.

[17] D. T. Hoang, D. Niyato, P. Wang, D. I. Kim, and Z. Han, "The tradeoff analysis in RF-powered backscatter cognitive radio networks," in *Proc. IEEE Global Commun. Conf. (GLOBECOM)*, Dec. 2016, pp. 1–6.

[18] R. Kishore, S. Gurugopinath, P. C. Sofotasios, S. Muhaidat, and N. Al-Dhahir, "Opportunistic ambient backscatter communication in RF-powered cognitive radio networks," *IEEE Trans. Cognit. Commun. Netw.*, vol. 5, no. 2, pp. 413–426, Jun. 2019.
[19] D. T. Hoang, D. Niyato, P. Wang, and D. I. Kim, "Optimal time sharing in RF-powered backscatter cognitive radio networks," in *Proc. IEEE Int. Conf. Commun. (ICC)*, May 2017, pp. 1–6.
[20] B. Lyu, H. Guo, Z. Yang, and G. Gui, "Throughput maximization for hybrid backscatter assisted cognitive wireless powered radio networks," *IEEE Internet Things J.*, vol. 5, no. 3, pp. 2015–2024, Jun. 2018.
[21] T. D. Tran and L. B. Le, "Hybrid backscatter and underlay transmissions in RF-powered cognitive radio networks," in *Proc. 26th Int. Conf. Telecommun. (ICT)*, Apr. 2019, pp. 11–15.
[22] S. H. Kim and D. I. Kim, "Hybrid backscatter communication for wireless-powered heterogeneous networks," *IEEE Trans. Wireless Commun.*, vol. 16, no. 10, pp. 6557–6570, Oct. 2017.
[23] B. Lyu and D. T. Hoang, "Optimal time scheduling in relay assisted batteryless IoT networks," *IEEE Wireless Commun. Lett.*, vol. 9, no. 5, pp. 706–710, May 2020.
[24] N. Van Huynh, D. T. Hoang, D. Niyato, P. Wang, and D. I. Kim, "Optimal time scheduling for wireless-powered backscatter communication networks," *IEEE Wireless Commun. Lett.*, vol. 7, no. 5, pp. 820–823, Oct. 2018.
[25] Y. Ye, L. Shi, X. Chu, and G. Lu, "Throughput fairness guarantee in wireless powered backscatter communications with HTT," *IEEE Wireless Commun. Lett.*, early access, Aug. 6, 2020, doi: 10.1109/LWC.2020.3014740.
[26] L. Shi, R. Q. Hu, J. Gunther, Y. Ye, and H. Zhang, "Energy efficiency for RF-powered backscatter networks using HTT protocol," *IEEE Trans. Veh. Technol.*, early access, Aug. 5, 2020, doi: 10.1109/TVT.2020.3014500.
[27] M. Song and M. Zheng, "Energy efficiency optimization for wireless powered sensor networks with nonorthogonal multiple access," *IEEE Sensors Lett.*, vol. 2, no. 1, pp. 1–4, Mar. 2018.
[28] H. Chingoska, Z. Hadzi-Velkov, I. Nikoloska, and N. Zlatanov, "Resource allocation in wireless powered communication networks with non-orthogonal multiple access," *IEEE Wireless Commun. Lett.*, vol. 5, no. 6, pp. 684–687, Dec. 2016.
[29] P. D. Diamantoulakis, K. N. Pappi, Z. Ding, and G. K. Karagiannidis, "Wireless-powered communications with non-orthogonal multiple access," *IEEE Trans. Wireless Commun.*, vol. 15, no. 12, pp. 8422–8436, Dec. 2016.
[30] J. Kimionis, A. Bletsas, and J. N. Sahalos, "Increased range bistatic scatter radio," *IEEE Trans. Commun.*, vol. 62, no. 3, pp. 1091–1104, Mar. 2014.
[31] J. Papandriopoulos and J. S. Evans, "SCALE: A low-complexity distributed protocol for spectrum balancing in multiuser DSL networks," *IEEE Trans. Inf. Theory*, vol. 55, no. 8, pp. 3711–3724, Aug. 2009.
[32] S. Boyd, *Convex Optimizarion*. Cambridge, U.K.: Cambridge Univ. Press, 2004.
[33] Q. Wu, W. Chen, D. W. Kwan Ng, J. Li, and R. Schober, "User-centric energy efficiency maximization for wireless powered communications," *IEEE Trans. Wireless Commun.*, vol. 15, no. 10, pp. 6898–6912, Oct. 2016.

WEN-GANG ZHOU received the B.Eng. degree in computational mathematics from Henan Normal University, in 1997, and the M.Eng. degree in computer application technology from the North China University of Technology, in 2007. He is currently pursuing the Ph.D. degree with the City University of Macau. He is currently a Full Professor with the School of Computer Science and Technology, Zhoukou Normal University. His research interests include RF energy harvesting-enabled wireless communications and intelligent algorithm design for wireless communications.